Museros Romero, P.; Andersson, A.; Pinazo, B. (2024). Dynamic behaviour of bridges under critical conventional and regular trains: Review of some regulations included in EN 1991-2. Proceedings of the Institution of Mechanical Engineers Part F Journal of Rail and Rapid Transit. 238(8):977-988. https://doi.org/10.1177/09544097241245150

Museros, Andersson and Pinazo 1Universitat Politècnica de València, Dpt. of Continuum Mechanics and Theory of Structures, Valencia, Spain
2KTH Royal Institute of Technology, Division of Structural Engineering and Bridges, Stockholm, Sweden Pedro Museros, Universitat Politècnica de València, Camino de Vera s/n, 46022 Valencia, Spain. pmuseros@mes.upv.es

Abstract

In the field of structural analysis dedicated to the study of vibrations of high-speed railway bridges, one reference load model is the well-known HSLM-A, which *limits of validity* are stated in Eurocode EN 1991-2, Annex E. In a recent paper published in the *Journal of Rail and Rapid Transit*, the authors investigated the degree of coverage provided by HSLM-A to *critical articulated trains*. Now in the present article, the authors have extended those analyses to *critical conventional and regular trains* as well. This is an important aspect because HSLM-A as such is an articulated-type model, so it is of interest to understand how it deals with covering the various resonance phenomena generated by other train types. Therefore, the main goal of this work is to establish whether the conventional and regular trains that stem from the validity rules given in Annex E/EN 1991-2, produce vibratory effects that are duly covered by HSLM-A. Following the aforementioned validity rules, one first aspect analysed is the importance of near-to-integer wheelbase ratios in the coupled vibrations produced by conventional trains. Subsequently, seven realistic, conventional and regular high-speed train models have been synthesised; these models have been made publicly available in *Mendeley Data*, and comprise almost 3800 different sequences of axle loads. Finally, the response of simply-supported bridges has been analysed with a view to compare the seven synthesised models vs HSLM-A. The *exceedance* and *required speed increase* have been computed for both displacements and accelerations, in a comprehensive ensemble of spans and speeds. The results provide a diagnosis of the degree of coverage of HSLM-A with respect to those conventional and regular trains compliant with Annex E/EN 1991-2.

load model, high-speed train, conventional train, regular train, train spectrum, cumulative acceleration, cumulative displacement, HSLM-A

Dynamic behaviour of bridges under critical conventional and regular trains: review of some regulations included in EN 1991-2

Pedro Museros1, Andreas Andersson2 and Benjamín Pinazo1

October 6, 2024

1 Introduction

As it is known, in high-speed bridge design the resonant response generated by normative load models will be determinant to assess the fulfilment of the suitable Ultimate Limit States (ULS) and Serviceability Limit States (SLS); see for instance the report from the expert committee [**?**]. Given that the European load model HSLM-A from standard [**?**] comprises ten vehicles, all of them of *articulated* type, it is of interest to analyse whether the theoretical resonances predicted under the action of HSLM-A will cover adequately the potential resonances generated by other vehicle types as well, particularly by *Conventional* and *Regular* high-speed trains.

In a recent article published in this journal by [**?**], the authors analysed the resonant effects of Articulated trains in a wide ensemble of simply supported bridges, with a view to establishing whether high-speed load model HSLM-A from [**?**] covers the dynamic response of those trains included within the so-called *limits of validity* of HSLM-A. Such limits of validity are stipulated in Annex E from [**?**] (in what follows, simply *Annex E*). The present article is a comprehensive extension of that previous publication, with the main purpose of analysing the coverage given by HSLM-A to both Conventional and Regular trains. For this reason, a brief synopsis of the main conclusions from the preceding paper is given first.

In [**?**], the authors followed an approach based on the concepts of *train signature* and *bogie factor* (known also as *bogie spectrum*), that proves convenient to explain why in a few particular cases load model HSLM-A is slightly non-conservative in the treatment of articulated trains (ATs). The results derived from extensive numerical simulations based on train signatures were subsequently confirmed by numerical time integration analyses. The most important findings, related to ATs, were the following:

- A new simplified expression of the train signature was developed for ATs. Using such new expression, it was found that the dynamic effects of ATs with ratios $\eta = D/d_{\mathrm{BA}}$ close to integer are not significantly more aggressive than those of ATs where η is far from integer (symbol D represents the car-body length of an AT, and d_{BA} is the wheelbase of its shared or *Jacobs* bogies). The possibility of η integer ratios being noticeably more

aggressive than non-integer ones is somewhat implicit in the text of Annex E, where it is stated that HSLM-A will not cover trains where η is close to integer. That conclusion was later confirmed for the range of speeds corresponding to first and second bogie resonances in a subsequent work by [**?**], and will be extended for Conventional trains (CTs) in next section, which is a significant achievement of this paper. As for Regular trains (RTs), this kind of vehicles have single axles between their car-bodies, and therefore potential coupling effects between carriages and bogies are not possible.

- In general the HSLM-A model covers well the vibration (acceleration) effects of ATs derived from Annex E for simply supported (S-S) concrete bridges of spans between 7–30 m. The effects in composite/steel bridges of spans between 15–50 m are also covered except for some very high frequency bridges. The analysis was restricted to bridges where the linear mass is not lower than 50% of $\hat{m}(L) = 400L + 4900$ kg/m, L being the S-S span in m.

- Both the general signature and time integration were used to analyse the coverage provided by HSLM-A to the Annex E ATs on S-S high-speed bridges, with tolerances of 10–15% in amplitude and 20% in speed. The minimum linear mass, as well as the load distribution due to the ballasted track, played a decisive role for finding relevant examples with accelerations above 3.5 m/s^2. Particularly for concrete structures of spans between 7–30 m, only two relevant examples of non-coverage were found, corresponding to spans $L \simeq 12.4$ m and $L \simeq 13$ m. In the remaining cases, HSLM-A covers the Annex E ATs as regarding the vertical accelerations.

Since the objective of this article is to complete and broaden the scope of the mentioned previous work, the literature review carried out for that article [**?**] is still relevant, but will not be repeated here for brevity. From the date of that publication, subsequent work was carried out in the framework of *In2Track2* project—within the *Shift2Rail* initiative. Many of the new developments presented here were conceived as tasks scheduled for [**?**].

In the framework of In2Track2 project (and subsequent In2Track3), also the German Railway Infrastructure Manager (DB Netz AG, recently renamed DB InfraGO AG) has pursued relevant investigations on the compatibility of railway vehicles and bridges. The German Federal Railway Authority (EBA) has also completed in 2023 a research project coordinated by *TU Darmstadt* and focused in this area, entitled "Bridge Dynamics; dynamic load model". Some of the outcomes of those research activities are discussed below.

One of them is the development of a five-level data model based on single beams with simple supports for the static and dynamic assessment of existing railway bridges, by G. [**?**]. In this recent paper, progressively refined analyses of a large database of filler beam bridges are proposed and described, from initial static compatibility checks related to the so-called *EN Line cathegories* (level 1), to very detailed experimental analyses under resonant conditions (level 5). The use of spectra in this approach is limited to train signatures, but the systematic adopted methodology will be certainly of interest to infrastructure managers, as well as to vehicle and bridge engineers. The presentation of all relevant information in one single, combined excitation-response diagram is one of the

useful features of this updated approach to the static–dynamic compatibility check of single-span superstructures of an entire network.

Within the above mentioned project funded by EBA, two publications have investigated various aspects of current European regulations on bridge dynamic analysis. [**?**] have presented a proposal of a new high-speed train load model for dynamic calculation of railway bridges. In this paper, a representative ensemble of 3150 real trains were collected; from an envelope of their dynamic excitation, 20 proposed, normative trains were fitted and gathered in the new load model, which was subsequently tested for 300 existing bridges. In line with the present paper, the work of [**?**] points out the need of an update of model HSLM-A, due to potential lack of coverage in certain cases.

Moreover, [**?**] have analysed in depth the so-called *Additional Damping* method proposed in [**?**] to reduce the vibratory effects induced by high-speed trains, particularly at resonance. This kind of research is complementary to investigations related to load models—as the present paper—, because the various proposals of Additional Damping are intended to be applied to the structural models of bridges, in order to moderate to some extent the resonance peaks predicted under such load models.

Also a further work that contributes to the analysis of bridge vibrations, particularly in terms of spectra is the recent publication from Auersch [**?**]. His approach in the frequency domain separates three factors in the solution: the spectrum of the modal force, the frequency response function of the bridge mode, and the axle-sequence spectrum of the train. Particular novelty in the work from Auersch is the analysis of resonances created by long freight trains, which produce low frequencies and high amplitudes of the car-length spectrum. This kind of methodology highlights the advantages of reasoning on the basis of spectra for better insight into the railway excitation, as it was employed previously by the authors [**?**] and will also be used in next section.

2 Effects of integer wheelbase ratios in conventional trains

As previously mentioned, Annex E prescribes a series of conditions or *limits of validity* of load model HSLM-A. Such limits place restrictions on the high-speed vehicles which dynamics effects on bridges are intended to be covered by HSLM-A. One of such limitations is that ratios $\eta = D/d_{\mathrm{BA}}$ and $\gamma = (d_{\mathrm{BS}} - d_{\mathrm{BA}})/d_{\mathrm{BA}}$ *should not be close to an integer value*. In this context d_{BS} is the wheelbase between centres of adjacent bogies across consecutive cars, see Figure **??**b.

It is difficult to establish a limit where η or γ can be considered close enough to an integer value, in such a way that a train no longer falls within the limits of validity of HSLM-A. Therefore, in this section we will consider three possibilities:

- *Case* 1: this is the case when η and/or γ are far from an integer value by no more than 0.1 in absolute value, as for instance $\eta = 6.07$ (with some margin left) or $\gamma = 1.9$ (no margin left).

- *Case* 2: this is the case when η and/or γ are far from an integer value by no more than 0.2 in absolute value, as for instance $\eta = 6.17$ or $\gamma = 1.8$.

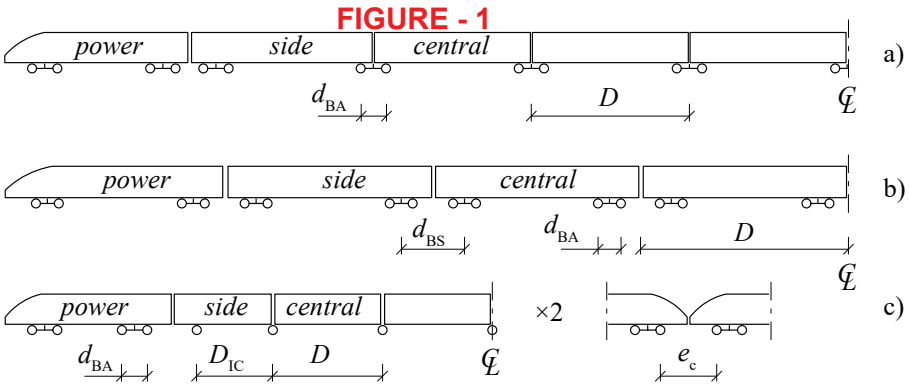

Figure 1: Schematic representation of different train types, a) an articulated train, b) a conventional train and c) a regular train.

- *Case* 3: this is the case when η and/or γ are far from an integer value by no more than 0.3 in absolute value, as for instance $\eta = 6.27$ or $\gamma = 1.7$.

In [**?**], it was demonstrated that the signature of a regular series of equidistant bogies can be computed as the product of the signature of a regular series of single, equidistant loads, times the *bogie factor*, which is a unique term that gathers the dynamic effect of the two loads in a bogie. Those two functions are repeated below for completeness.

The mathematical expression of the signature of a set (train) of k equidistant unit loads that travel at distance D is

$G_E(k, \Lambda, \zeta) = k$ if $\zeta = 0$ and $\Lambda = 1, 1/2, 1/3, ...$

$G_E(k, \Lambda, \zeta) = \sqrt{\sigma^{2(1-k)} f_k(\sigma, \Lambda) f_1(\sigma, \Lambda)}$ otherwise.

where $\Lambda = \lambda/D$ is the nondimensional wavelength, $\lambda = VT$ is the wavelength, V is the train speed and T is the period of vibration of the mode shape that is excited by the moving loads. Also in equation eq:signature$_r egular_t rain$,$\sigma = e^{\zeta 2\pi/\Lambda} \geq 1$, ζ is the damping ratio, and function f_k is defined as

$$f_k(\sigma, \Lambda) = (1 + \sigma^{2k} - 2\sigma^k \cos(2k\pi/\Lambda)) \tag{1}$$

where $f_1 = f_k(k = 1)$. The bogie factor can be written as a function of various parameters; adopting $b = d_{\mathrm{BA}}$ for brevity, the most convenient form in this context is

$$f_B(b, \lambda, \zeta) = \sqrt{1 + e^{-\zeta 4\pi b/\lambda} + 2e^{-\zeta 2\pi b/\lambda} \cos(2\pi b/\lambda)} \tag{2}$$

With these mathematical bases, the signature of a CT can be written easily by realising, Figure **??**b, that the effects of the two bogies in one carriage can be combined by means of a so-called *car factor* f_C, analogous to the bogie factor f_B:

$$f_C(r, \lambda, \zeta) = \sqrt{1 + e^{-\zeta 4\pi r/\lambda} + 2e^{-\zeta 2\pi r/\lambda} \cos(2\pi r/\lambda)} \tag{3}$$

where $r = D - d_{\mathrm{BS}}$ is the inner bogie wheelbase. Therefore, the signature of a conventional train where all loads have identical values P is obtained by multiplication of P times equations eq:signature$_r egular_t rain, eq : bogie_f actorandeq : car_f actor.Orsimply, forunitloa$

$$G_{CT}(\lambda, \zeta, D, b, r, k) = G_E(k, \lambda/D, \zeta) \times f_B(b, \lambda, \zeta) \times f_C(r, \lambda, \zeta) \qquad (4)$$

Equation eq:signature$_c$*onventional*$_t$*rainisaconciseyetcomprehensiveexpressionthatallowstoexploretheir* and different levels of damping. This will be carried out below, with a view to considering four different possibilities:

- all possible realistic combinations (D, b, r) included,
- combinations (D, b, r) that verify *Case* 1 are removed,
- combinations (D, b, r) that verify *Case* 2 are removed,
- combinations (D, b, r) that verify *Case* 3 are removed.

With this strategy, it will be clarified whether the peak dynamic effects of realistic CTs where η and γ ratios can take any value, including integers or near-integers, are significantly more aggressive than realistic CTs where integer or near-integer η and γ are removed, in the three mentioned levels, Case 1, 2 and 3. In this regard, it is important to consider values of (D, b, r) from actual fast trains. Since $r = D - d_{\mathrm{BS}}$, distance d_{BS} is preferable to collect relevant data as it is done in Table **??**, where the information for 20 CTs designed for speeds $\geq$ 200 km/h is shown. Such data have been collected either from published technical literature, or received directly from infrastructure managers. The trains are sorted on ascending value of D.

Some interesting conclusions can be extracted from Table **??**. There is no clear relation between D and d_{BA}, but in general d_{BS} increases with D as expected; however, the ratio d_{BS}/D does not feature clear trends either. Values of d_{BS}/D are contained approximately within the interval 0.26–0.33; therefore, that range will define the realistic limits considered in all analysis presented here for CTs. Also of interest is to notice that integer or near-integer ratios η and γ are found in quite a few cases. This implies that vehicle manufacturers do not always discard such near integer ratios when designing their fast trains. Notice that two entries are given for ICE-4, since two different wheelbases are used for the bogies of such train.

The analyses in this section is based on the following parameter ranges:

- $17 \leq D \leq 31$ m, in steps of 0.05 m
- $2.3 \leq d_{\mathrm{BA}} \leq 3.5$ m, in steps of 0.01 m
- $0.26 \leq d_{\mathrm{BS}}/D \leq 0.33$, in steps of 0.005
- two cases of modal damping, ζ=1% and ζ=3%
- two cases of number of carriages, $k = 13$ and $k = 24$
- wavelengths $2 \leq \lambda \leq 32$ m, in steps of 0.01 m.

The upper range for D is to consider the car lengths of future trains. For d_{BA}, the lower limit is taken from Table **??** and the upper limit from Annex E. The number of cars is selected to make a total train length of about 400 m for $k = 14$ with $D = 31$ m and $k = 24$ with $D = 17$ m.

Figure **??** shows the results for $\zeta = 1.0\%$ and $k = 24$ carriages. As it can be seen, Case 1 and 2 present a very small reduction in the amplitude of the

Table 1: Data from actual conventional trains for speeds $\geq$ 200 km/h.

Train	D**(m)**	d_{BA}**(m)**	η	d_{BS}**(m)**	γ	d_{BS}/D
Javelin 395	20.000	2.60	7.69	5.82	1.238	0.2910
EN 1991-2, Annex D-1	20.300	2.60	7.81	6.20	1.385	0.3054
MU Network Rail	23.000	2.60	8.85	7.60	1.923	0.3304
VIRGIN	23.900	2.70	8.85	6.90	1.556	0.2887
ICE-3	24.775	2.50	9.91	7.40	1.960	0.2987
X-2000	24.960	2.90	8.61	7.26	1.503	0.2909
SKS-300	25.000	2.50	10.00	7.50	2.000	0.3000
Pioneer	25.500	2.50	10.20	7.50	2.000	0.2941
China-Star	25.500	2.56	9.96	7.50	1.930	0.2941
ICE-T BR 411	25.900	2.70	9.59	6.90	1.556	0.2664
Alfa Pendular	25.900	2.90	8.93	6.90	1.379	0.2664
ICE TD, BR 605	26.020	2.60	10.01	7.02	1.700	0.2698
ETR-Y-500	26.100	3.00	8.70	7.10	1.367	0.2720
EN 1991-2, Annex F-D	26.200	3.00	8.73	7.20	1.400	0.2748
ICE 1, BR 401	26.400	2.50	10.56	7.40	1.960	0.2803
ICE-2	26.400	2.50	10.56	7.40	1.960	0.2803
I11	26.400	2.56	10.31	8.00	2.125	0.3030
ET 403	27.160	2.60	10.45	8.16	2.138	0.3004
ICE-4 (1)	28.750	2.30	12.50	9.25	3.022	0.3217
ICE-4 (2)	28.750	2.60	11.06	9.25	2.558	0.3217

signature: though we have removed the triplets (D, b, r) that yield η and γ very close to integer, little has changed. Even in Case 3, which removes 60% of all potential values of η and γ, the reduction in the signature is not large, approximately 15% in the range of $\lambda \simeq 3$ m, where the largest difference is observed. Similar conclusions are reached for the other values of damping and k considered here; they are not shown for the sake brevity.

It can be concluded that the maximum coupling effects due to near integer ratios η and γ are not significantly larger than the vibrations created by other non-integer ratios, when considering realistic triplets (D, b, r) along with representative values of damping and number of carriages. Maximum signature peaks do not diminish more than some 15%, even when 60% of triplets (D, b, r) are removed around the integer η and γ values (*i.e.* Case 3). This results are consistent with the actual wheelbases employed in various types of CTs, where near integer ratios coexist with other ratios far from integer, see Table **??**.

3 Definition of realistic conventional and regular HS vehicles: train signatures

From the data and results in the previous section, it does not seem justified to exclude η and γ ratios close to integer from the analysis of CTs. This conclusion will be now taken into account in a subsequent procedure where an extensive

FIGURE - 2

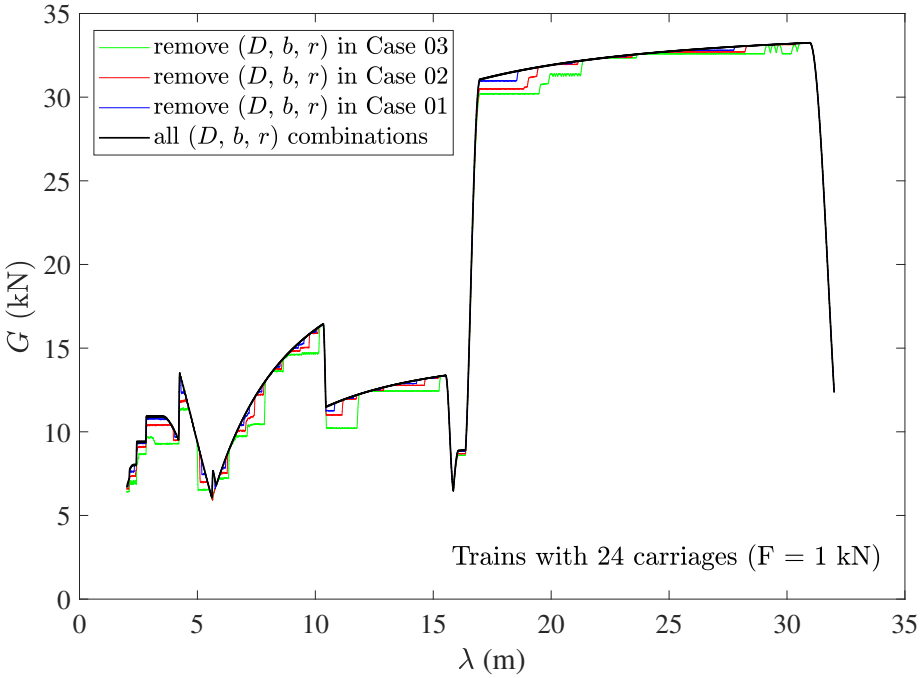

Figure 2: Comparison of signature of CTs for various cases of near integer (η, γ) ratios. $\zeta = 1.0\%$

set of realistic CTs and RTs will be derived from Annex E in EN 1991-2. The restrictions contemplated for defining such trains are summarised below. The resulting data are publicly available in a Mendeley repository [**?**]. These trains will be used in the two next sections for comparison of dynamic effects vs HSLM-A; for that reason, in order to keep the computational cost under reasonable limits, the discretization of parameters is coarser than in previous section.

3.1 Realistic conventional trains from Annex E

Following the conditions stipulated in Annex E, the CTs defined for use in this paper are as follows:

- Car-body length in the range $18 \leq D \leq 27$ m.
- Axle load P below 170 kN.
- Total length below 400 m.
- Total weight below 10000 kN.
- Bogie wheelbase within $2.5 \leq d_{\mathrm{BA}} \leq 3.5$ m.
- Axle load P limited by equation E.2 from Annex E, which states the following:

$$4P\cos\left(\frac{\pi d_{\mathrm{BS}}}{D}\right)\cos\left(\frac{\pi d_{\mathrm{BA}}}{D}\right) \leq 2P_{\mathrm{HSLMA}}\ \cos\left(\frac{\pi d_{\mathrm{HSLMA}}}{D_{\mathrm{HSLMA}}}\right) \tag{5}$$

where P_{HSLMA}, d_{HSLMA} and D_{HSLMA} are parameters corresponding to the Universal Trains of HSLM-A, corresponding to coach length D_{HSLMA} for: (a) a single Universal Train where D_{HSLMA} equals the coach length D of a real CT; or (b) two Universal Trains where D_{HSLMA} does not equals D with D_{HSLMA} taken as just greater than D and just less than D.

Based on these conditions stipulated in Annex E, along with Table **??** for realistic d_{BS}/D ratios, the discretization of train wheelbases is carried out as follows. Range of D is: $18 \leq D \leq 27$ m, in steps of 1.0 m; also, $0.26 \leq d_{\mathrm{BS}}/D \leq 0.33$ in steps of 0.01; regarding the d_{BA} range $2.5 \leq d_{\mathrm{BA}} \leq 3.5$ m, in steps of 0.25 m. The axle load is always taken as high as possible, fulfilling the conditions mentioned above.

Moreover, four models with different types of traction have been considered for the CTs: (1) distributed traction, *i.e.* no power cars present, and patterns of axle distances identical for all coaches (thus, all coaches in each train are identical); (2) power cars with a wheelbase distribution identical to the locomotives of HSLM-A, *i.e.* 0–3–11–3–3.125 m; (3) power cars with a wheelbase distribution identical to the locomotives of S103 unit from RENFE (an Alsthom high-speed train), *i.e.* 0–2.5–14.875–2.5–4.9 m; (4) power cars with a wheelbase distribution identical to the locomotives of S112 unit from RENFE (Talgo Avril), *i.e.* 0–2.8–8.2–2.8–4.276 m. These four different tractions represent four families or load models that are referred to as follows for convenience:

Model 101 with distributed traction; **model 102** with HSLM-A-like power cars; **model 103** with S103-like power cars; **model 104** with S112-like power cars. Due to the discretization of D, d_{BA} and d_{BS}, each model has a total of 400 trains.

It should be emphasised that previous Eq. eq:equation$_E$2$_f$rom$_A$nnexEisaconditionthatimposesthatthefo harmonic)thanthetrainsinHSLM−Awithasimilarcarriagelength D. Figure **??**, wherethedampedsignature Aareshown, demonstratesthatEq. eq : equation$_E$2$_f$rom$_A$nnexEisindeedeffectiveinkeepingthoseCTsignat Aenvelope, forallwavelengthsoffirstsub−harmonics(18.0≤ λ ≤ 27.0 m). Conversely, such coverage fails for the third and higher sub-harmonics ($\lambda < 9.0$ m), which is the main reason why, in the following sections, it will be found that the CTs produce higher accelerations and displacements than HSLM-A for those relatively low wavelengths.

It can also be seen that the envelope of the curves matches well with the shape of the theoretical signature in Figure **??**, with much more refined discretization. One final conclusion is that the type of traction has a not too large influence, and most times distributed traction convoys produce the strongest vibrations, for the same or very similar total length.

3.2 Realistic regular trains from Annex E

Following the conditions stipulated in Annex E, the RTs considered in this paper are as follows:

- car-body length $10 \leq D \leq 14$ m
- axle load P below 170 kN

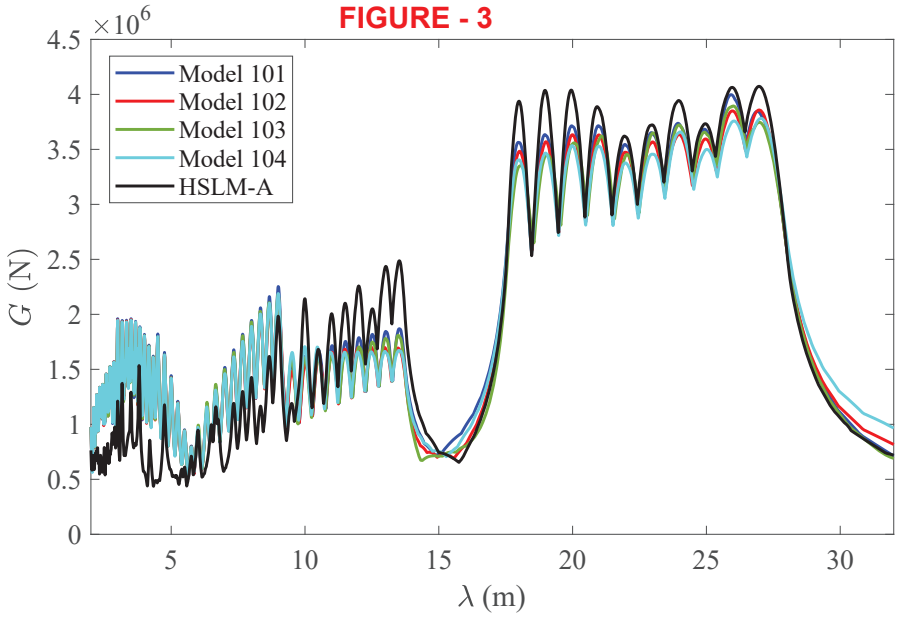

Figure 3: Signatures of HSLM-A and CT load models 101–104, 1% damping.

- total length below 400 m
- total weight below 10000 kN
- intermediate coach length $8 \leq D_{\mathrm{IC}} \leq 11$ m
- train set coupling distance $7 \leq e_{\mathrm{c}} \leq 10$ m.

Regular high-speed trains of length up to 400 m are usually double units, see Figure **??**c. That assumption will be followed here, with D_{IC} and e_{c} belonging to the ranges mentioned above. As for the CTs, axle load is always taken as high as possible, fulfilling the above conditions. The parameters D, D_{IC} and e_{c} are varied in steps of 0.5 m.

Analogously to the definition of CTs, three models with different types of traction have been considered for the RTs (distributed traction is not usual in RTs): **Model 301** with HSLM-A-like power cars; **model 302** with S103-like power cars; **model 303** with S112-like power cars. Each of these models has a total of 441 trains.

The signatures of these three load models are shown in Figure **??**, along with HSLM-A, for 1% damping. As it can be seen, areas of non-coverage are distributed in certain intervals for wavelengths below $\lambda = 14$ m, and quite continuously in the range $4 \leq \lambda \leq 7$ m. Being double units, the influence of power cars in the dynamic response is more visible, particularly for $\lambda \geq 11$ m and $\lambda \leq 3.6$ m.

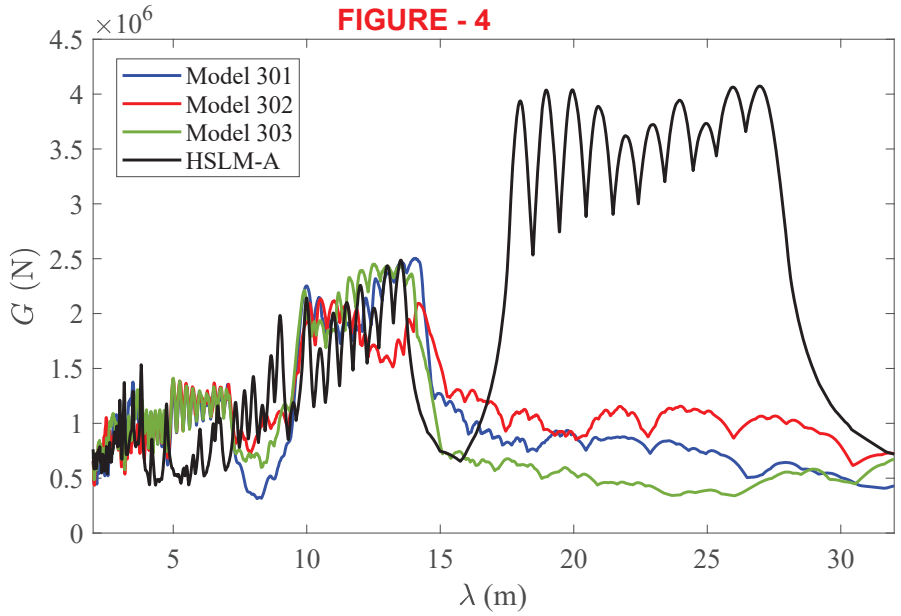

Figure 4: Signatures of HSLM-A and RT load models 301–303, 1% damping.

3.3 Normative load model HSLM-A: summary of characteristics

For the sake of completeness, the main characteristics of load model HSLM-A are summarised below. Detailed information regarding this load model can be obtained from section 6.4.6.1.1 in [**?**].

- Comprises 10 normative trains of articulated type.
- Car-body length in the range $18 \leq 27$ m, in steps of 1 m.
- Axle load P constant for each train, varying between 170 kN and 210 kN.
- Total length of each train close to 400 m.
- Bogie wheelbase constant in each train, varying within $2.0 \leq d_{\mathrm{BA}} \leq 3.5$ m.
- Symmetric end power cars with an axle distance pattern of 0–3–11–3–3.525 m.

4 Methodology for bridge dynamic analysis

The dynamic analysis of the bridges employed here to investigate the potential lacks of coverage of HSLM-A, both for CTs and RTs, is carried out following the same basic principles adopted in [**?**]. Those principles are summarised in this section.

Bridges of S-S type are considered, with spans $4\,\mathrm{m} \leq L \leq 20\,\mathrm{m}$, in steps of 0.10 m. Their linear mass is given by equation (**??**), which can be considered

a reference lower bound for S-S railway bridges. The use of a low but realistic mass is important because high linear masses would hinder relevant results by delivering too low acceleration response values, below the meaningful threshold of 3.5 m/s^2.

$$\hat{m}(L) = 400L + 4900 \quad \text{(kg/m) with } L \text{ in (m)} \tag{6}$$

Structural damping follows EN 1991-2 table 6.6 and depends on bridge type and span length: for a span length of 4–20 m the damping varies linearly from 2.5–0.5% for composite bridges and 2.1–1.0% for pre-stressed concrete bridges. For longer spans the damping is constant and equal to the lower values.

A realistic low value is assumed for the first natural frequency of the structures. To this end, the lower bound of EN 1991-2 figure 6.10 is adopted. Such low frequencies, in combination with a speed range $50-400$ km/h (in steps of 1.0 km/h) ensure that all relevant resonant peaks will be suitably captured. When considering the results plots in next sections, it should be however taken into account that speeds higher than 250 km/h would not be typical for S-S spans below some 15 m (approx.), because in modern high-speed lines those shorter spans tend to be covered with stiff portal frames.

The time integration is carried out using Duhamel's integral, based on a moving point forces approach. For the purpose of comparing directly various load models (*i.e.* normative $\equiv$ HSLM-A vs. realistic trains), vehicle-bridge interaction effects will be neglected.

Longitudinal axle load distribution through the sleepers and ballast needs to be taken into account to eliminate non-realistic high levels of vibration for the lower wavelengths. The reduction coefficient proposed by [**?**] and [**?**] is therefore employed here. A recent work by [**?**] confirms that such mitigation effect at low wavelengths is of importance and should be considered in the analyses.

With a view to compare the principal resonant response induced by load model HSLM-A *vs.* realistic trains, only the fundamental mode of vibration is considered in the time integration. Moreover, [**?**] have proved the existence of an equivalent filtering effect due to longitudinal axle load distribution that will affect more strongly the higher modes (due to their correspondingly shorter wavelengths), and further mitigate their potential contributions.

5 Comparison of dynamic effects from different trains: Definition of *Exceedance* and *Required speed increase*

The comparison of the CT and RT load models defined in previous section vs HSLM-A is carried out following the same principles as in [**?**]. To this end, two indicators referred to as *exceedance* and *required speed increase*, defined in this section, are used in order to verify whether the dynamic response of simple bridges under a given CT/RT load model is adequately covered by HSLM-A or not.

It should be emphasised that the comparisons are performed here in terms of *cumulative* response, given that the operating speed of one track section may be reduced to lower values for particular reasons. Therefore, for a given design speed of the line V, the highest peak response at any speed lower than V is determinant for bridge design. Figure **??** is used to explain this concept.

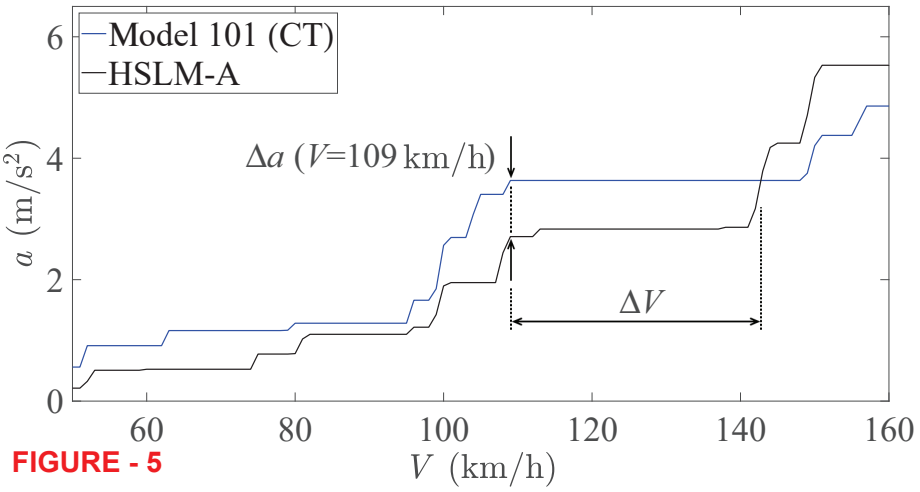

FIGURE - 5

Figure 5: Cumulative response in acceleration for a bridge of span $L = 25.2\,\mathrm{m}$: definition of exceedance Δa and required speed increase ΔV.

Figure **??** shows that the cumulative response in terms of acceleration —the same applies to displacements— is marked by "steps", where the various trains from the Model 101 and the HSLM-A create successive resonant or sub-resonant peaks. So, each new peak causes a higher step in the cumulative response.

From an analysis as shown in figure **??**, first the *exceedance* in acceleration is defined —for each speed V— as $\Delta a(V) = \max\left[100\, a_{max,\mathrm{REAL}}(V) - a_{max,\mathrm{HSLMA}}(V) a_{max,\mathrm{HSLMA}}(V); 0\right]$

were subscript REAL implies that response is computed for a load model of a "real" train, *i.e.* either a CT or RT load model. The definition given in equation eq:exceedance$_d$*efinitionaboveappliestoverticaldisplacementsaswellbysimplyreplacingeach*a(V)*by*$\delta(V)$.

If a exceedance $\Delta a(V = V_0)$ or $\Delta\delta(V = V_0)$ is found to be below an acceptable limit, that acceleration or displacement in excess of the response computed with HSLM-A is not deemed relevant. Following [**?**], a threshold of 10% will be considered here.

Conversely, if $\Delta a(V = V_0) > 10\%$, the *required speed increase* ΔV is then computed as follows, for the vertical accelerations (the treatment of displacements is identical). The situation where $\Delta a(V = V_0) > 10\%$ does not necessarily imply by itself that the CT/RT load model is not duly covered; the important reason behind it is that the effects of HSLM-A may increase strongly for V only slightly larger than V_0 and, in such situation, the safety factor "design speed"/"operational speed" > 1 would suffice for HSLM-A to exceed the real train again. That situation can be observed in figure **??**, for instance, at speed $V = 100\,\mathrm{km/h}$.

Therefore, the predicted speed increase required for HSLM-A to cover a real train ΔV is defined as the minimum difference in speed (as a percentage) that is needed to reach, from the dominant peak of the real train response, the response curve of the HSLM-A with identical amplitude, but at higher speed. Figure **??** also illustrates that concept: in that example, the required speed increase at $V = 109\,\mathrm{km/h}$ is $(143 - 109)/109 = 0.31 \rightarrow \Delta V = 31\%$.

Finally it is important to mention that a speed increase ΔV is not considered

relevant below 20%, following the prescriptions of Eurocode EN 1991-2. Such code establishes that the standard increase of design speed to be assigned to HSLM-A model for bridge dynamic analysis is precisely 20%.

In summary, figure **??** shows an example where the exceedance $\Delta a(V = 109\,\text{km/h})$ is clearly above 10%, and such neat exceedance is maintained during an ample interval of speed, from 109 to 143 km/h. Since $\Delta V = 31\%$, the required speed increase is above 20% and the lack of coverage in this situation is relevant.

6 Exceedance analysis of conventional trains vs HSLM-A in S-S bridges

The principles for comparison of real trains *vs.* load models established in the previous section are now applied to investigate the CTs derived from Annex E in EN1991-2.

Most times, a real train will exceed the response of HSLM-A due to some resonance phenomenon that happens at speed lower than an equivalent or stronger resonant peak due to HSLM-A. Should this happen in the displacement response of a simple beam, it would entail a potential lack of coverage regarding the *impact coefficients* or *dynamic enhancement* (section 6.4.6.5 in [**?**]), which is related to the ultimate limit state analysis of the bridge. For that reason, it is preferable to consider all cases where relevant exceedance ($> 10\%$) in displacements occur, and evaluate its associated speed increase as it is done in figure **??** below. Conversely, for the acceleration analysis it is preferable to remove the cases where vibrations are not relevant enough for compromising bridge serviceability; therefore, in the following plots where $\Delta a > 10\%$ and its associated ΔV will be represented, as in figure **??**, every case where the vertical acceleration is below 3.5 m/s^2 is removed by setting directly $\Delta a = 0$. Track irregularity effects through coefficient φ'' in [**?**] are taken into account for computing the maximum acceleration.

It should be recalled that the mass level will not influence the displacement exceedance response, given that compared results vs HSLM-A will be presented. As for the accelerations, values somewhat lower than $\hat{m}(L)$ could be adopted for the steel/composite bridges, as it was discussed in [**?**]; that would increase the number of cases where the acceleration is above the threshold 3.5 m/s^2, but it will be seen from the results in here that the main conclusions of this article would not vary significantly even if the linear mass were below $\hat{m}(L)$. It should also be noted that the lower limit of natural frequency was used, corresponding to $n_{0,\min}$ in EN 1991-2. Therefore, the speeds where non-coverage occurs are low and sometimes below 200 km/h, but they would be proportionally higher if the actual bridge frequencies were higher. With this conceptual framework, the following exceedance and speed increase plots are presented and discussed.

First, the displacement exceedance for composite/steel bridges is shown in figure **??** for the CT load models 101–104, following figure **??**b. Large areas of exceedance in displacement are found, mainly for $\lambda < 10$ m, in agreement with the signature in figure **??**. The right subplot shows two regions where the required speed increase is higher than 20%, for $\lambda \approx 5$ m with a span length of 8–10 m and $\lambda \approx 6$–8 m with a span length of 12–16 m. For the lower bound

frequency this occurs at a train speed of about 150 km/h.

FIGURE - 6

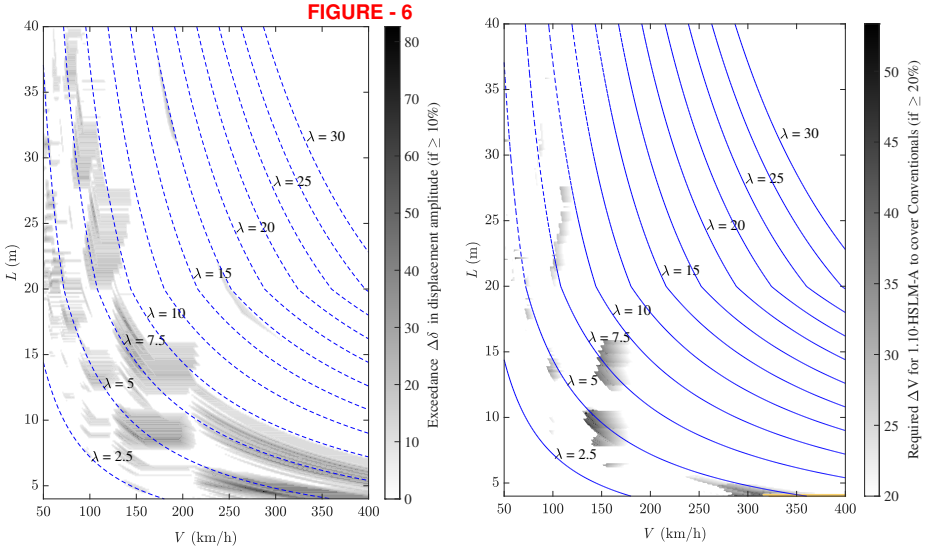

Figure 6: Exceedance in displacement and required speed increase for HSLM-A to cover the conventional load models 101–104. Single span steel/composite bridges.

Similar trend is found for accelerations, for steel/composite bridges in figure **??** and for pre-stressed bridges in figure **??** . Acceleration exceedance is found for $\lambda < 10$ m and span length up to about 25 m. The speed exceedance occur at even lower speeds, in some cases as low as 100 km/h and span length up to 25 m.

In summary, from these numerical simulations it can be concluded that HSLM-A does not adequately cover the displacement and acceleration response of single-span bridges traversed by conventional trains derived from Annex E, for wavelengths below 10 m, as it could be anticipated from the signatures shown in Figure **??**.

7 Exceedance analysis of regular trains vs HSLM-A in S-S bridges

Similar analyses are performed for the regular trains, denoted load models 301–303 and following figure **??**c. The exceedance in displacement is presented in figure **??** for steel/composite bridges. The displacement exceedance follow similar trend as for the CT, but in less scattered areas. Most important are two regions; $\lambda = 12.5$ m with $L = 33$ m and $\lambda = 5$ m with $L = 10$ m; both occurring at $V = 150$ km/h when using $n_{0,\min}$.

The acceleration exceedance is presented in figure **??** for steel/composite bridges and in figure **??** for pre-stressed concrete bridges. Both cases follow similar trends, but more pronounced for steel/composite bridges. For the pre-stressed concrete bridges the two most important regions are $\lambda = 5$–7.5 m with $L = 8$–14 m and $\lambda = 15$ m with $L = 28$ m. For steel/composite bridges additional

FIGURE - 7

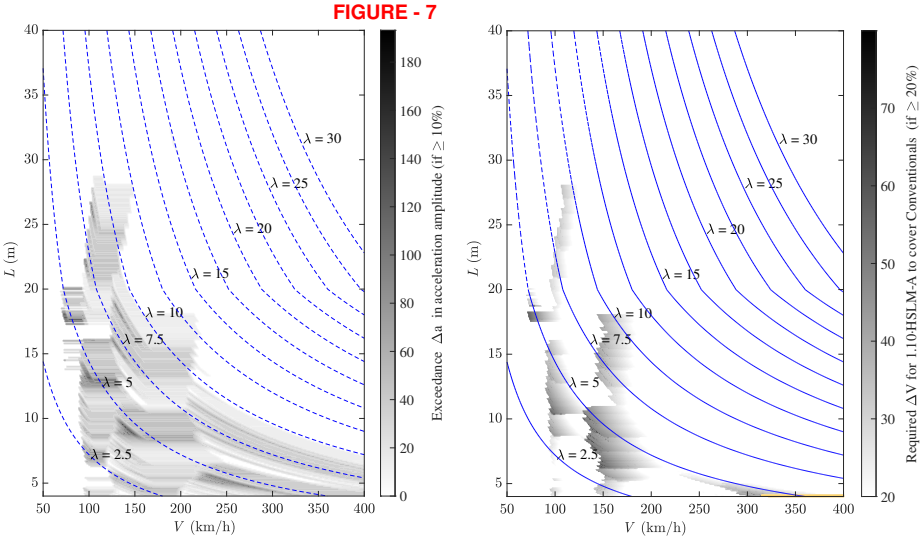

Figure 7: Exceedance in acceleration and required speed increase for HSLM-A to cover the conventional load models 101–104. Single span steel/composite bridges.

three regions appear; $\lambda = 5$–7.5 m with $L = 15$–20 m, $\lambda = 12.5$ m with $L = 22$ m and $\lambda = 12.5$ m with $L = 31$–35 m. The largest exceedance magnitude is found for $\lambda = 5$–7.5 m, in agreement with the signature presented in figure **??**.

In the above results both displacement and acceleration exceedance for both CT and RT are also found for $L < 10$ m. This area is not deemed critical for several reasons. Firstly the speed increase is mostly less than 20%, secondly the critical speed is generally higher than 200 km/h in combination with $n_{0,\min}$ and thirdly these structures are generally not built on high-speed lines.

8 Conclusions

Following the principles established in a previous article published in 2021 in the *Journal of Rail and Rapid Transit* [**?**], which was dedicated to the analysis of critical articulated trains, the authors have extended here those analyses to *critical conventional and regular trains*. The main goal of this work has been to establish whether the conventional and regular trains that stem from the *limits of validity* of load model HSLM-A—given in Annex E from EN 1991-2—produce a dynamic response in simple bridges, in terms of vertical displacements and accelerations, that is covered by the response predicted for the HSLM-A.

First, the effect of near-to-integer wheelbase ratios $\eta = D/d_{\mathrm{BA}}$ and $\gamma = (d_{\mathrm{BS}} - d_{\mathrm{BA}})/d_{\mathrm{BA}}$ of conventional trains has been investigated. This is one of the aspects mentioned in Annex E from EN 1991-2. From actual rolling stock data, it has been confirmed that such integer or nearly integer values of η and γ do exist in several real, high-speed vehicles. Moreover, using an analytical approach based in a new mathematical expression of the train signature, it has been confirmed that the response predicted is not significantly larger when η and γ are close to integer: considering thousands of different wheelbases of

FIGURE - 8

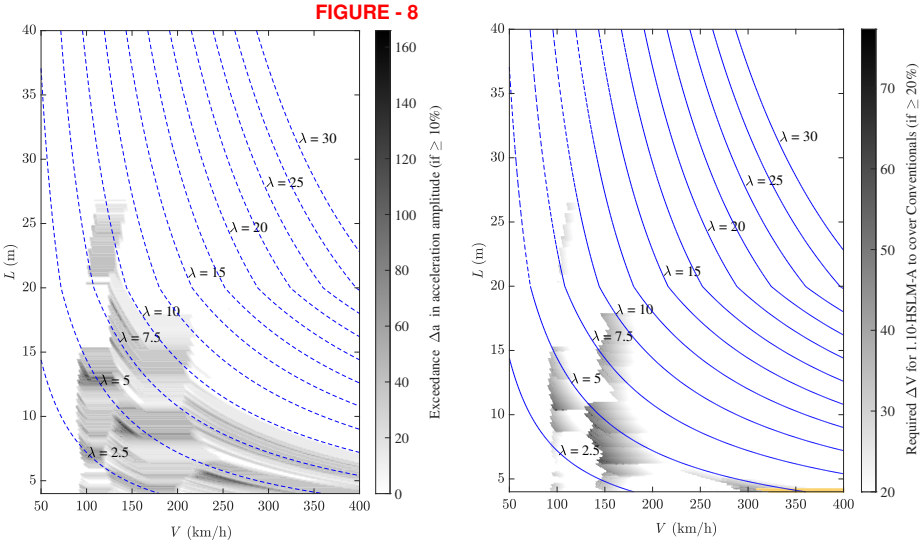

Figure 8: Exceedance in acceleration and required speed increase for HSLM-A to cover the conventional load models 101–104. Single span pre-stressed bridges.

conventional trains in a wide sensitivity analysis, it has been found that the maximum signature peaks do not diminish more than some 15%, even when as much as 60% of the realistic combinations of wheelbases are removed—precisely the ones that fall closer to integer η and γ values.

For these reasons, conventional trains where η and γ are integer or nearly integer have not been excluded from the subsequent analyses. The next step has been to derive seven realistic conventional and regular train models, with different types of power cars, that respect all prescriptions of Annex E from EN 1991-2—except η and γ being far from integer. Those train models, which comprise almost 3800 different sequences of axle loads, have been made publicly available in a Mendeley Data repository [**?**].

Finally, the response of simply-supported bridges has been analysed following the methodology in [**?**], with a view to compare the seven synthesised load models vs HSLM-A. The *exceedance* and *required speed increase* have been computed for both displacements and accelerations, in a comprehensive ensemble of spans from 4–40 m, and speeds up to 400 km/h. Realistic low bounds of frequency, linear mass and damping have been adopted for the bridges. A tolerance of 10% has been accepted for the exceedance, and 20% for the speed increase as in [**?**]. With this approach, the numerical simulations indicate that the HSLM-A does not cover adequately the displacement and acceleration response in some wavelength ranges, where the conventional and regular trains derived from Annex E/EN 1991-2 produce a higher response. That lack of coverage largely takes place at wavelengths that can be predicted from the signatures of the seven synthesised load models.

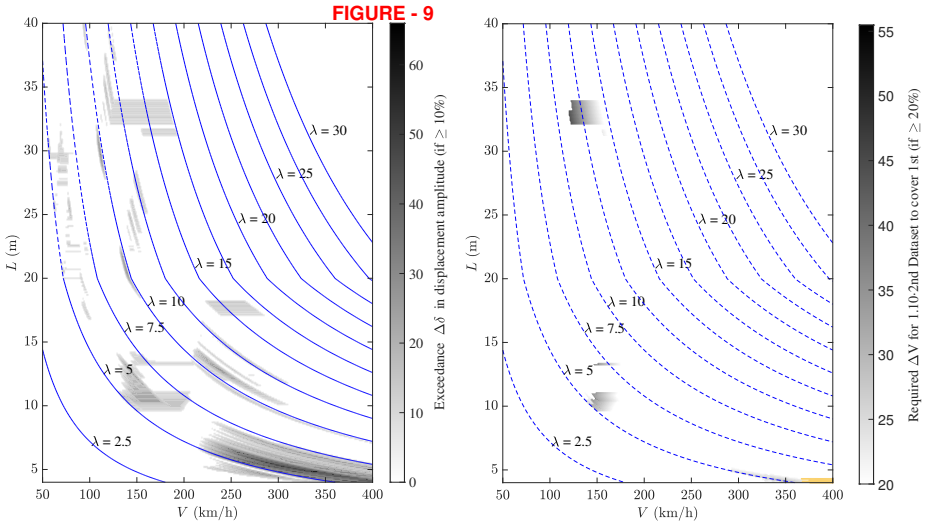

Figure 9: Exceedance in displacement and required speed increase for HSLM-A to cover the regular load models 301, 302 and 303. Single span steel/composite bridges.

9 Acknowledgements

This project has received funding from the European Union's Horizon 2020 research and innovation programme under Grant Agreement No 101012456. The content of this paper does not reflect the official opinion of the Europe's Rail Joint Undertaking (EU-Rail JU). Responsibility for the information and views expressed in the paper lies entirely with the authors.

References

[ERRI D214.2(2002)] European Rail Research Institute (D-214.2 Committee, ERRI D-214.2). *Use of universal trains for the dynamic design of railway bridges. Summary of results of D-214.2.* 2002.

[Museros et al.(2021a)] Museros P., Andersson A., Martí V. and Karoumi R. *Dynamic behaviour of bridges under critical articulated trains: Signature and bogie factor applied to the review of some regulations included in EN 1991-2.* P I Mech Eng F-J Rai, 2021; 235(5):655-675.

[EN 1991-2(2003)] European Committee for Standardisation (CEN). EN 1991-2.*Eurocode 1: Actions on structures. Part 2: General Actions – Traffic Loads on Bridges.* September 2003.

[Museros et al.(2021b)] Museros P., Andersson A. and Karoumi R. *Dynamic effect of trains with articulated coaches and Jacobs bogies with integer wheelbase ratios.* XI International Conference on Structural Dynamics, EURODYN 2020 (Athens); 2646-2657.

FIGURE - 10

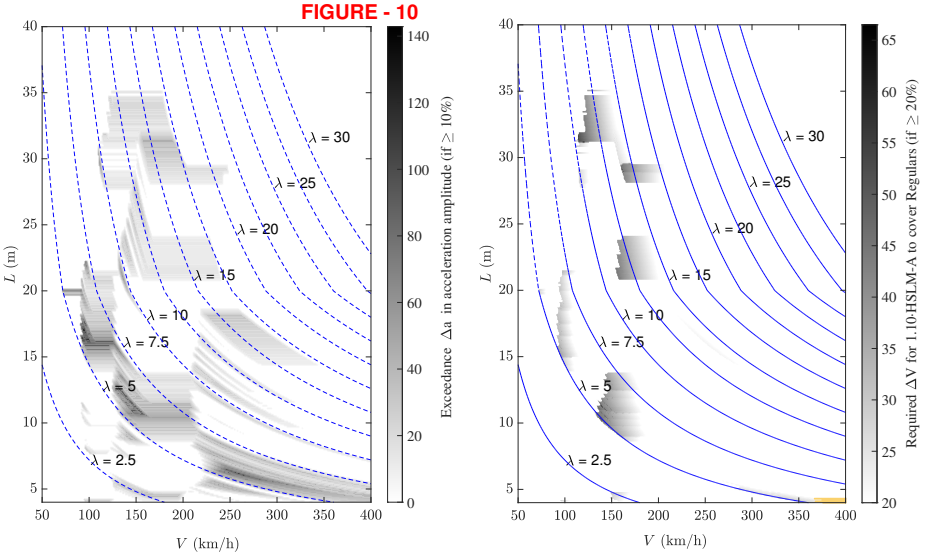

Figure 10: Exceedance in acceleration and required speed increase for HSLM-A to cover the regular load models 301, 302 and 303. Single span steel/composite bridges.

[In2Track2 Final Report(2021)] KTH Royal Institute of Technology, University of Porto, Polytechnic University of Valencia. *High speed low cost bridges, background report d5.2.5. In2Track2.* 2021.

[Grunert(2022)] Grunert G. *Data and evaluation model for the description of the static–dynamic interface between trains and railway bridges* Engineering Structures 2022; 262:114335.

[Reiterer et al.(2023)] M. Reiterer, M. Kwapisz, A. Firus, M. Rupp and G. Lombaert, *Development of a new high-speed train load model for dynamic calculation of railway bridges.* CE/papers Proceedings in Civil Engineering **6**(5) (2023) 422–429.

[Kohl et al.(2023)] A. M. Kohl, K.D. Clement, J. Schneider, A. Firus and G. Lombaert, *An investigation of dynamic vehicle-bridge interaction effects based on a comprehensive set of trains and bridges*, Engineering Structures 2023; 279:115555.

[Auersch(2021)] Auersch L. *Resonances of railway bridges analysed in frequency domain by the modal-force-excitation, bridge-transfer and axle-sequence spectra* Engineering Structures 2021; 249:113282.

[Museros et al.(2022)] Museros P., Andersson A., Pinazo B. *High-speed trains derived from Annex E / EN 1991-2*, Mendeley Data, V3, 2023 doi: 10.17632/hdr6dd5xv2.3

[ERRI D-214 RP9(1999)] European Rail Research Institute (D-214 Committee, ERRI D-214). *Rail bridges for speeds > 200 km/h. Final report (RP9).* 1999.

FIGURE - 11

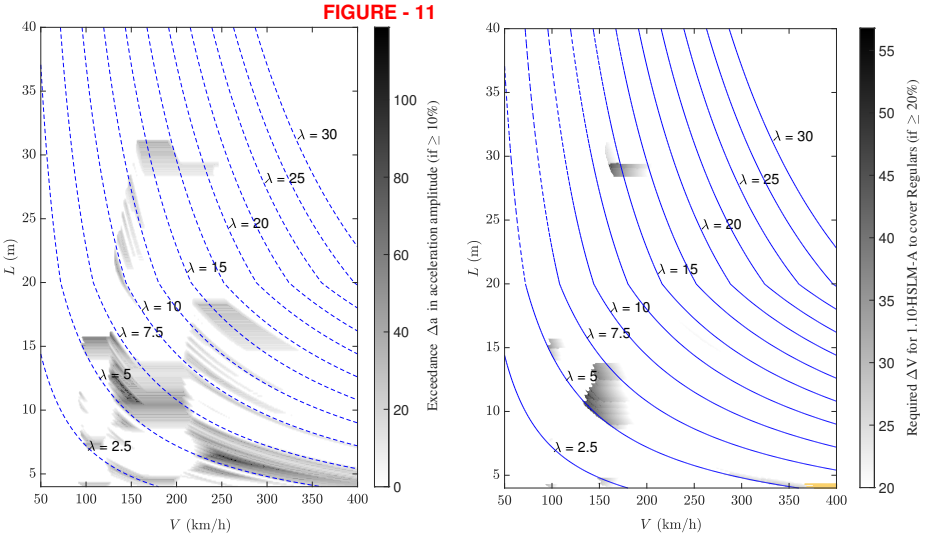

Figure 11: Exceedance in acceleration and required speed increase for HSLM-A to cover the regular load models 301, 302 and 303. Single span pre-stressed bridges.

[UIC 776-2R Leaflet(2003)] Union Internationale des Chemins de Fer. *UIC Code 776-2R: Design requirements for rail bridges based on interaction phenomena between train, track, bridge and in particular, speed.* 2003.

[Bettinelli et al.(2023)] L. Bettinelli, A. Stollwitzer and J. Fink, *Numerical study on the influence of coupling beam modeling on structural accelerations during high-speed train crossings.* Appl. Sci. (2023) 8746. doi: 10.3390/app13158746

[Jin et al(2005)] Jin Z., Huang B., Ren J. and Pei S. *Reduction of vehicle-induced vibration of railway bridges due to distribution of axle loads through track.* Shock Vib., 2018; Article ID 2431980.